

Radiation properties of cavity Čerenkov radiation

Ju Gao* and Fang Shen

Electrical and Computer Engineering Department, University of Illinois, Urbana, Illinois 61801, USA

(Received 22 December 2005; published 5 April 2006)

Čerenkov radiation from cavities has been analyzed by quantum electrodynamic theory. Analytical expressions of basic radiation properties such as the Einstein's A and B coefficients are derived and shown to be directly modified by the cavities. The analysis leads to the conclusion that the coherent radiation from the Čerenkov radiation devices is due to super radiance of spontaneous emission instead of stimulated emission. Coherent and incoherent radiations are analyzed in the THz radiation range.

DOI: [10.1103/PhysRevA.73.043801](https://doi.org/10.1103/PhysRevA.73.043801)

PACS number(s): 42.50.Ct, 03.70.+k, 41.60.Bq, 41.60.-m

I. INTRODUCTION

A free traveling electron emits photons spontaneously when its speed u is greater than the phase velocity v_p of the photon it emits. Such process can occur in a dielectric medium [1,2] and is known as Čerenkov radiation (CR). Since its discovery, Čerenkov radiation has played an important role in high energy physics for detecting particles [3]. The broad spectrum of CR has also stimulated thoughts [4] of using it as a radiation source, particularly in a frequency range difficult of access by other means. High frequency microwave radiations in the hundreds of GHz range have been generated in dielectrically loaded CR devices [5,6] where a vacuum tunnel is typically used inside the dielectric for the electrons to travel and a metal cavity is also used to confine the radiation field. Here the topic is revisited because there have been much interests recently in generating practical THz radiation, which ranges between 300 GHz to 30 THz in frequency. What makes THz radiation particularly interesting is the natural match of the frequency band to the molecular vibrational and rotational energy bands, leading to potential applications in chemistry, biology, and astronomy, etc. The simplicity of the radiation scheme, mature technology of fabricating dielectric structures, and the possibility of integrating field emission electron sources [7] present CR device as yet another alternative to the pursuit of submillimeter or THz radiation, in parallel to synchrotrons [8], free electron lasers [9], optically-pumped molecular lasers [10], quantum-cascade lasers [11], and femtosecond laser-pumped photoconductive antennas [12].

Analysis of the CR devices [13–19] are mostly treated by classical electrodynamics, where the electron motion is governed by the Newton-Lorentz equation and the radiation as a result of the moving electron is ruled by the Maxwell equations. The treatment is justified for the lower frequency range. In the higher frequency range, from infrared (IR) to ultraviolet (UV), quantum theory gives a more accurate description of quantum electronics devices such as lasers. Since THz radiation is an extension of IR, quantum mechanical treatment for the radiation is adequate and even required. In

this paper, we will analyze the basic radiation properties of the CR devices. For example, we will calculate the Einstein's A and B coefficients and show how the cavity affects their value. We will also analyze the incoherent and coherent radiations from the device.

II. EINSTEIN'S A COEFFICIENT FOR CR IN A UNIFORM DIELECTRIC MEDIUM

We begin with deriving the Einstein's A coefficient in a uniform dielectric medium. In the quantum view, the process is described as a photon generated by the electron with energy and momentum conservation,

$$(E_{p'}, \mathbf{P}') + (\hbar\omega, \hbar\mathbf{k}) = (E_p, \mathbf{P}), \quad (1)$$

where (E_p, \mathbf{P}) and $(E_{p'}, \mathbf{P}')$ are the four momenta of the electron before and after the process, respectively, with $E_p = \sqrt{\mathbf{P}^2 + m^2}$ and $E_{p'} = \sqrt{\mathbf{P}'^2 + m^2}$. ω and \mathbf{k} are the photon frequency and wave vector, respectively. The process can be illustrated by a diagram as shown in Fig. 1. Notice a photon cannot be generated in the vacuum according to Eq. (1).

The ability to radiate is measured by the Einstein's A coefficient, a concept introduced even before the full repertoire of quantum mechanics was developed. A is equivalent to the transition probability rate

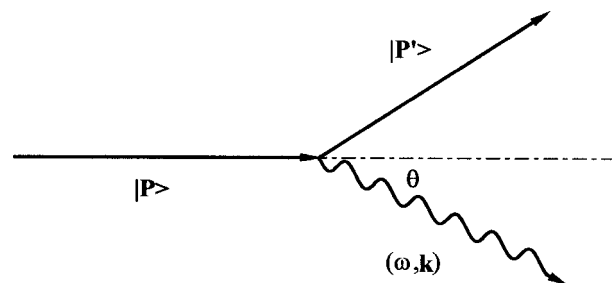


FIG. 1. A Čerenkov photon of frequency ω and wave vector \mathbf{k} is generated by the transition of free electron from $|\mathbf{P}\rangle$ state to $|\mathbf{P}'\rangle$ state, where \mathbf{P} and \mathbf{P}' represent the electron momenta before and after the radiation.

*Electronic address: jugao@uiuc.edu

$$\begin{aligned}
 A &= 2\pi |H_{int}|^2 \delta(E_{P'}/\hbar + \omega, E_P/\hbar) \\
 &= 2\pi \left(\frac{1}{\hbar}\right)^2 |\langle 1 | \langle \mathbf{P}' | c\alpha \cdot \mathbf{A}(\mathbf{k} \cdot \mathbf{r}) | \mathbf{P} \rangle | 0 \rangle|^2 \delta(E_{P'}/\hbar + \omega, E_P/\hbar),
 \end{aligned}
 \tag{2}$$

where H_{int} is the transition matrix and δ function enforces the resonant condition. $|\mathbf{P}\rangle = \frac{1}{\sqrt{V}} e^{i\mathbf{P}\cdot\mathbf{r}} u(\mathbf{P})$ and $|\mathbf{P}'\rangle = \frac{1}{\sqrt{V}} e^{i\mathbf{P}'\cdot\mathbf{r}} u(\mathbf{P}')$ are the electron wave functions before and after the radiation. V is the normalization volume and $u(\mathbf{P})$ and $u'(\mathbf{P})$ are the Dirac spinors. A photon is generated, $|0\rangle \rightarrow |1\rangle$, by the interaction $c\alpha \cdot \mathbf{A}(\mathbf{k} \cdot \mathbf{r})$ in which dipole approximation is not used. α is a Dirac matrix and $\mathbf{A}(\mathbf{k} \cdot \mathbf{r})$ is the quantized radiation field given by

$$\mathbf{A}(\mathbf{k} \cdot \mathbf{r}) = g(\epsilon \hat{a} e^{i\mathbf{k}\cdot\mathbf{r}} + \epsilon^* \hat{a}^\dagger e^{-i\mathbf{k}\cdot\mathbf{r}}),
 \tag{3}$$

where \hat{a} and \hat{a}^\dagger are the creation and annihilation photon operators, respectively. $e^{i\mathbf{k}\cdot\mathbf{r}}$ represents the plane wave photon field with, however, the dispersion relationship is $k = n\frac{\omega}{c}$ where n is the index of refraction of the medium. $g = \sqrt{\frac{\hbar}{2\epsilon V_\gamma \omega}}$ is the field normalization constant where V_γ is the normalization volume of the field.

The analytical expression of the Einstein's A coefficient for the CR in the uniform medium is readily carried out by integrating Eq. (2) over all \mathbf{k} s and \mathbf{P}' s, where the radiation angle is derived to be frequency dependent due to electron recoil, $\cos \theta = \frac{1}{\beta n} + \frac{\hbar k}{2P} (1 - \frac{1}{n^2})$, and uniform dispersion of the medium is assumed

$$A = \alpha \beta \frac{E_P}{\hbar} F(\beta, n),
 \tag{4}$$

where $\alpha = \frac{e^2}{4\pi\epsilon_0\hbar c}$ is the fine structure constant and $\beta = u/c$, where u is the electron speed. $F(\beta, n)$ is an explicit function of β and n

$$\begin{aligned}
 F(\beta, n) &= \left(\frac{7}{4\beta^2} + \frac{1}{4\beta^2 n^2} - 2\right) + \left(\frac{3}{8\beta^2} + \frac{1}{8\beta^2 n^2} - \frac{1}{2}\right) \eta_m \\
 &+ \left(\frac{7}{4\beta^2} + \frac{5}{4\beta^2 n^2} - 3\right) \ln(1 - \eta_m) / \eta_m,
 \end{aligned}
 \tag{5}$$

where $\eta_m \equiv \frac{\hbar\omega_m}{E_P}$ and ω_m is the maximal radiation frequency

$$\hbar\omega_m = 2\frac{\beta n - 1}{n^2 - 1} E_P < \frac{2}{n + 1} E_P < E_P.
 \tag{6}$$

Equation (6) shows that the electron cannot convert its entire energy to a radiating photon, in contrast to the classical theory that claims infinite maximum frequency. If we allow ω_m to be infinite and neglect the electron recoil, we recover the classical expression of the Čerenkov radiation power with N_e electrons

$$P = A\hbar\omega N_e = \frac{e^2 N_e}{4\pi\epsilon_0 c} \beta \int_0^\infty \omega d\omega (1 - \cos^2 \theta).
 \tag{7}$$

To appreciate the value of the A coefficient, let the material be quartz so $n = \sqrt{3.78} = 1.944$ and $\beta = 0.634 > 1/n$. The maximal photon frequency is $\omega_m = 1.7 \times 10^{20}$ rad s⁻¹ accord-

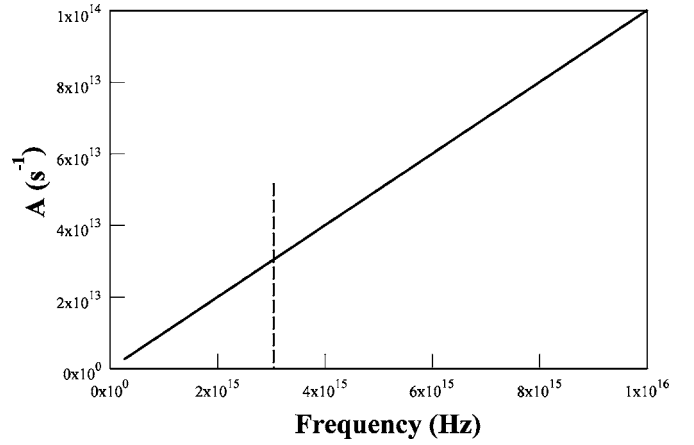


FIG. 2. Einstein's A coefficient values as a function of the cutoff wavelength for $n=1.944$ and $\beta=0.634$.

ing to Eq. (6). In reality, the medium becomes absorptive at such high frequency, thus cutoff frequency of CR is much smaller. Figure 2 shows A value as a function of the cutoff frequency. Suppose the cutoff wavelength is 100 nm, we show $A \approx 3 \times 10^{13}$ s⁻¹. Notice here the large A value represents a wideband of radiation while a typical atomic A is only for a narrow line of radiation.

III. EINSTEIN'S A AND B COEFFICIENTS FOR CAVITY ČERENKOV RADIATION

It is desirable for many applications to have the radiation energy concentrated in a narrow and discrete band, which requires discrete energy levels of the radiation system. The free electron does not possess discrete energy levels for discrete radiations, but the alternative is to force discrete fields by a cavity so that the electron can only lose its energy to those fields. A cavity CR device has thus been formed by enclosing the dielectric with a conducting material [6,20] as shown in Fig. 3, where a vacuum tunnel is built for the electrons to travel. We will study the structure illustrated by Fig. 3 as a basic cavity CR device.

The fields that can survive inside the cavity is called eigenmode fields that have a special dispersion relationship derived to be

$$\frac{I_1(Xa)}{I_0(Xa)X} = -\frac{\epsilon[Y_1(Ya)J_0(Yb) - J_1(Ya)Y_0(Yb)]}{\epsilon_0 Y[J_0(Ya)Y_0(Yb) - Y_0(Ya)J_0(Yb)]},
 \tag{8}$$

where J_n is the n th order Bessel function and I_n and Y_n are the n th order modified Bessel function of the first and second

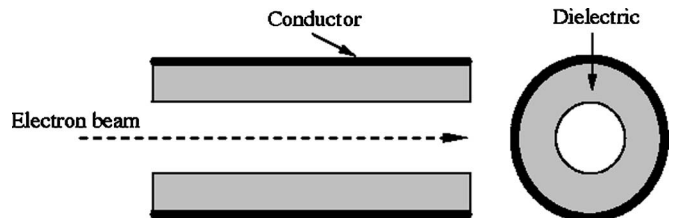


FIG. 3. A typical dielectric lined cavity CR device illustrates a conducting tube with radius b and a vacuum tunnel with radius a .

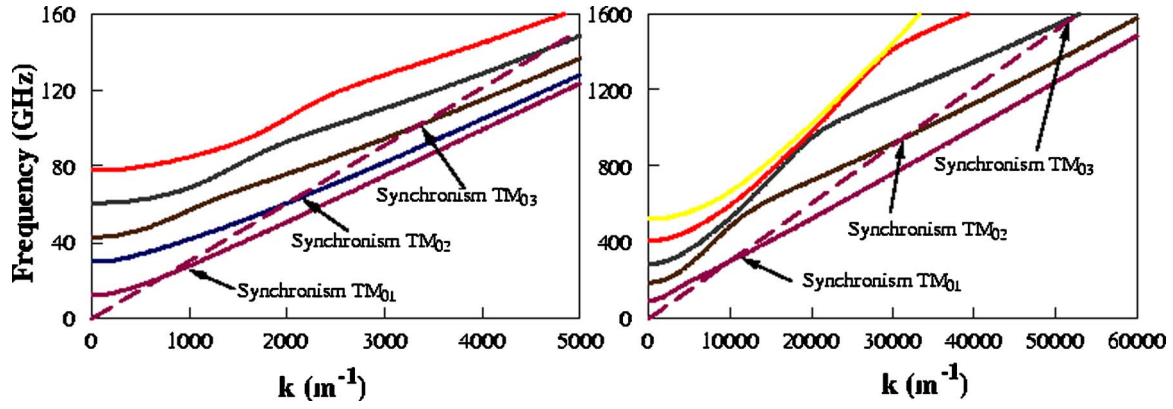


FIG. 4. (Color online) Dispersion curves for the different modes in two different cavity CR devices: (left) $a=3$ mm, $b=6$ mm; (right) $a=1.0$ mm, $b=1.2$ mm. Both have $\epsilon=3.78\epsilon_0$ and $\beta=0.634$. The dotted line represents the linear dispersion that gives phase velocity of βc .

kind. $X=k^2 - (\frac{\omega}{c})^2$ and $Y = \frac{\epsilon}{\epsilon_0} (\frac{\omega}{c})^2 - k^2$ are separation constants. Equation (8) is obtained by solving the Maxwell equations using the boundary conditions that (a) the tangential component of the electric field is continuous and (b) the tangential component of the magnetic field is continuous.

Figure 4 plots the dispersion relationships expressed by Eq. (8) for two different cavity structures. The first cavity is used in the experiments [6,20], and the second cavity is smaller designed for higher frequencies. Only transverse magnetic (TM) modes are considered because they dominate the interaction $\mathbf{P} \cdot \mathbf{A}$.

The mode characteristic alone does not fixate discrete frequencies. Additional relation comes from energy-momentum conservation conditions between the photon and the electron described by Eq. (1). Since here $\mathbf{k} \parallel \mathbf{P}$ and $\mathbf{P}' \parallel \mathbf{P}$, we have

$$v_p \equiv \frac{\omega}{k} = \frac{\beta c}{1 + \frac{\eta}{2} \left[\left(\frac{kc}{\omega} \right)^2 - 1 \right]} \approx u - u \frac{\eta}{2} \left[\left(\frac{1}{\beta} \right)^2 - 1 \right], \quad (9)$$

where $\eta = \hbar \omega / E_p$. Equation (9) is combined with Eq. (8) to give the actual, discrete radiation frequencies. Notice that the electron velocity and the field velocity do not match exactly

due to electron recoil, which may explain that the radiation frequency is slightly higher than the synchronism frequencies as observed in experiments [20]. Figure 4 illustrates the synchronization points as the interception between the dispersion curve and the $\omega/k = \beta c$ line, where it is shown that some frequencies are already in the THz range for the smaller cavity.

The cavity not only selects certain field modes but causes the field distribution to deviate from the plane wave. Because the transition rate depends on the overlap between the field function and the electron wave function [Eq. (2)], the modified field distribution can dramatically change the radiation properties. This effect has been studied extensively as a subject of cavity QED. For example, it has been observed that the spontaneous emission rate is modified from that in vacuum [21]. The uniqueness here is that the radiators are the free electrons instead of atoms, molecules, and even nuclei. The dielectric medium is necessary for the free electrons to radiate in the cavity.

The quantized radiation field inside the cavity is derived following the standard quantization procedure of radiation fields [22]. The derived quantized field is different from that in Eq. (3), where the plane wave function as the solution to the Helmholtz equation $\nabla^2 \mathbf{A} - \partial^2 \mathbf{A} / \partial t^2 = 0$ in vacuum is replaced by the solution in the cavity.

$$\mathbf{A}(\mathbf{r}) = \mathbf{z} g' (\hat{a} e^{ikz} + \hat{a}^\dagger e^{-ikz}) \times \begin{cases} I_0(X\rho), & \rho \leq a \\ \frac{\epsilon_0 Y}{\epsilon X} \left[\frac{I_1(Xa) J_0(Yb) Y_0(Y\rho) - I_1(Xa) Y_0(Yb) J_0(Y\rho)}{Y_1(Ya) J_0(Yb) - J_1(Ya) Y_0(Yb)} \right], & a < \rho \leq b. \end{cases} \quad (10)$$

The normalization coefficient g' in Eq. (10) is derived to give the total Hamiltonian $\hat{H} = \frac{1}{2} \hbar \omega (\hat{a} \hat{a}^\dagger + \hat{a}^\dagger \hat{a})$

$$g' = \sqrt{\frac{\hbar}{2\epsilon L \pi b^2 \omega} f}, \quad (11)$$

$$f \equiv \sqrt{\frac{2\epsilon_0 \pi b^2}{\mu_0 \int_0^a H_1^2 2\pi \rho d\rho + \epsilon_0 \int_0^a E_1^2 2\pi \rho d\rho + \mu \int_a^b H_{11}^2 2\pi \rho d\rho + \epsilon \int_a^b E_{11}^2 2\pi \rho d\rho}},$$

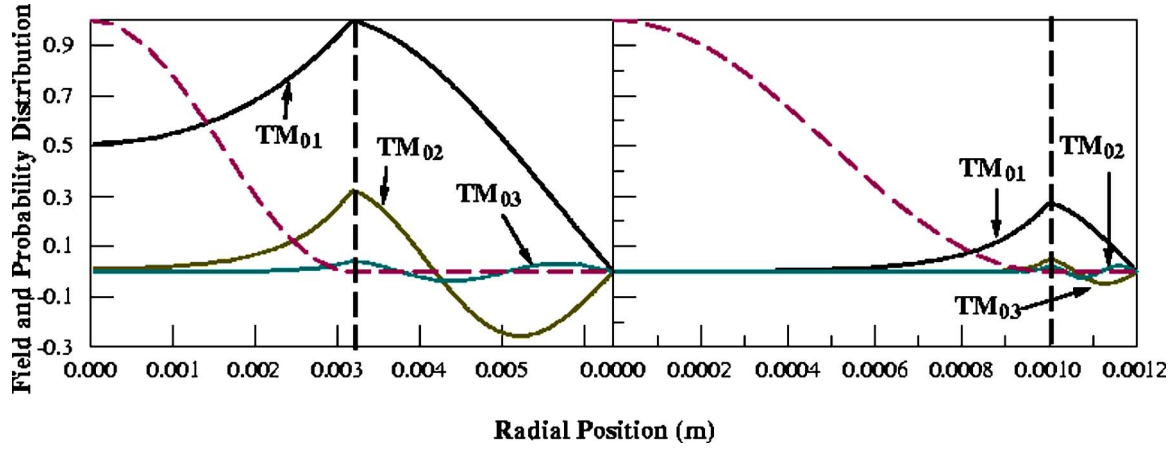


FIG. 5. (Color online) The A field functions (solid lines) are plotted along with the electron probability distributions (dashed line) inside the two cavities: (left) $a=3.175$ mm, $b=6.35$ mm; (right) $a=1.0$ mm, $b=1.2$ mm.

where L is the cavity length and H_I, E_I and H_{II}, E_{II} are the magnetic and electric fields in the tunnel ($\rho \leq a$) and dielectric ($a < \rho \leq b$) regions, respectively, given explicitly by

$$E_I = iI_0(X\rho),$$

$$H_I = \frac{\omega\epsilon_0}{X} I_1(X\rho),$$

$$E_{II} = i \frac{\epsilon_0}{\epsilon X} \frac{Y I_1(Xa) J_0(Yb) Y_0(Y\rho) - I_1(Xa) Y_0(Yb) J_0(Y\rho)}{Y_1(Ya) J_0(Yb) - J_1(Ya) Y_0(Yb)},$$

$$H_{II} = \frac{\omega\epsilon_0}{X} \frac{I_1(Xa) J_0(Yb) Y_1(Y\rho) - I_1(Xa) Y_0(Yb) J_1(Y\rho)}{Y_1(Ya) J_0(Yb) - J_1(Ya) Y_0(Yb)}. \quad (12)$$

The normalized field functions are plotted in Fig. 5 together with the electron wave functions that is also confined by the cavity as well. The difference is that the dielectric wall is the only boundary for the electrons assuming there is no tunneling into the dielectric medium. The lowest order electron wave function is then

$$|\mathbf{P}\rangle = \begin{cases} \frac{e^{iPz/\hbar} u(P)}{\sqrt{L}} \frac{J_0(2.405\rho/a)}{a\sqrt{\pi} J_1(2.405)} & (\rho < a) \\ 0 & (\rho > a). \end{cases} \quad (13)$$

The corresponding electron probability distribution is plotted in Fig. 5. A narrower electron distribution can be described by the superposition of a few higher order electron wave functions. The electron energy and momentum are practically unchanged by the cavity because the dimension of the radial confinement is too large so that $\Delta P_\rho \sim \hbar/\Delta\rho \ll P$.

The A coefficient is then calculated by using the new wave function [Eq. (13)] and field [Eq. (10)], and the analytical expression is found again

$$A_{cav} = \alpha\beta^2(1 + \eta) f^2 F^2 \frac{c^2}{(2\pi)^2 b^2 \omega_0 v_g} \frac{2c}{v_g}, \quad (14)$$

where ω_0 is the synchronism frequency and F is the filling factor that measures the overlap between the field and the electron wave function

$$F = \int_0^a \frac{1}{a^2 \pi J_1^2(2.405)} J_0^2(2.405\rho/a) I_0(X\rho) 2\pi\rho d\rho, \quad (15)$$

and $v_g = \left. \frac{d\omega}{dk} \right|_{\omega_0}$ is the group velocity at the synchronism frequency.

The A_{cav} is shown to be determined by the cavity geometry and the dielectric material. That means in practice its value can be engineered through the cavity design. Again the concept here draws analogy to that in cavity QED where the radiation phenomena are modified by the cavities.

The Einstein's B coefficient can also be derived from QED by calculating the transition rate from N_γ existing photons to $N_\gamma + 1$ photons

$$2\pi \left(\frac{1}{\hbar} \right)^2 |\langle N_\gamma + 1 | \langle \mathbf{P}' | c\boldsymbol{\alpha} \cdot \mathbf{A}(\mathbf{k} \cdot \mathbf{r}) | \mathbf{P} \rangle | N_\gamma \rangle|^2 \times \delta(E_{P'}/\hbar + \omega, E_P/\hbar) = B_{cav,emi} \rho_\gamma, \quad (16)$$

where N_γ is the photon number in the mode and ρ_γ is the corresponding photon density. Equation (16) gives the Einstein's B coefficient for emission. The B coefficient for absorption can also be found by assuming photons go from N_γ to $N_\gamma - 1$. Thus we have

$$B_{cav,emi} = N_\gamma \alpha \beta^2 (1 + \eta) f^2 F^2 c^3 / (b^2 \omega_0) I,$$

$$B_{cav,abs} = N_\gamma \alpha \beta^2 (1 - \eta) f^2 F^2 c^3 / (b^2 \omega_0) I. \quad (17)$$

Notice that the two B s are not exactly the same and the emission coefficient is only slightly bigger than the absorption one, which suggests that the device can be used as an amplifier where the stimulated emission should exceed the simulated absorption.

TABLE I. A coefficient at different frequency for Walsh's cavity.

Mode	Frequency (GHz)	A (s^{-1})
TM ₀₁	21.9	1.07×10^7
TM ₀₂	60.7	4.53×10^5
TM ₀₃	101.5	2.07×10^3

IV. NUMERICAL EXAMPLES AND DISCUSSION

Numerical values of the cavity coefficient A_{cav} can be calculated according to Eq. (14). Tables I and II list the A_{cav} values calculated for the two cavity designs. The electron energy is chosen to be 100 KeV, a value used in the experiments. The result shows that the higher order modes own the smaller A values, but these A values are generally higher than the typical A values for atoms or molecules at the same frequency range. There are two main reasons for that fact: first the cavity helps to confine the radiation field so that the overlap between the field and the electron wavefunction is enhanced; second the electron momentum is much larger than the electron momentum inside an atom. The latter contributes to the A coefficient due to the fact that the interaction is proportional to $\mathbf{P} \cdot \mathbf{A}$, where \mathbf{P} is the electron momentum [which is expressed by the operator $c\alpha$ in Eq. (2)].

As shown by Eq. (14), A_{cav} is proportional to ω^{-1} , which indicates that scaling up the frequency of the cavity microwave devices results in weaker radiation. In the same time, notice that the atomic A coefficient in the open space is proportional to ω^3 , which also shows the unfavorable tendency of scaling down the frequencies of the visible or IR devices. This is one of the contributing factors of the difficulty in generating THz radiation that is falling in the gap between the microwave and IR radiation.

Now that we have calculated the A and B coefficients, we are ready to discuss coherent radiations from quantum mechanical perspective. Electrons in a monoenergetic beam are in the excited state described by $|\mathbf{P}\rangle$. Stimulated emission can occur by the electrons making transition to the lower states, e.g., $|\mathbf{P}'\rangle$. This is clearly a case of population inversion since the lower states are empty. However the allowable higher states are empty also to which the electron can make a transition by absorbing a photon. Therefore population inversion alone does not ensure net stimulated emission since the process is proportional to $(B_{emi} - B_{abs})IN_e$, where I is the intensity of the radiation field. Equations (17) show that $(B_{emi} - B_{abs}) \propto \eta \equiv \hbar/E_p \ll 1$, therefore only minute gain in the amplified stimulated emission process. This effect is confirmed by the experiments [6,20] in which a second cavity CR device is used as an amplifier and small gain is observed. The conclusion is that the amplified stimulated emission or lasing is not responsible for the coherent radiation from this type of devices.

We now turn our attention to another coherent radiation generation mechanism. Coherent radiation can indeed be

TABLE II. A coefficient at different frequency for the designed cavity.

Mode	Frequency (GHz)	A (s^{-1})
TM ₀₁	296	1.07×10^6
TM ₀₂	944	6.48×10^2
TM ₀₃	1601	1.88×10^1

generated by the spontaneous radiation from radiators, if the occupying space dimension is much smaller than the radiation wavelength. The phenomenon has been analyzed [23] even before the advent of laser and is known as the super radiance or super radiation. In super radiation, the radiators interact with the vacuum fields of the same phase thus the amplitudes of the transition matrix elements for all radiators are added so that the power is proportional to the square of the number of radiators. The effect has been well studied for atoms which are immobile compared to the speed of light. For electron devices, the electrons need to be grouped together while traveling, and process is known as bunching. A bunched beam has the output power proportional to the square of the bunched electrons, $P = A_{cav} \hbar \omega N_e^2$. The electrons can be both prebunched as in experiment [5] or self-bunched during the interaction as in experiments [6,20], which is true for many other free electron radiation devices. As an example for THz radiation generation, assuming $A = 6.48 \times 10^2 s^{-1}$ for the TM₀₂ mode in the smaller device (Table II), we find that 5×10^7 bunched electrons in the cavity is needed to give 1 mW power from the device. The current level for that number of electrons corresponding to the electron speed of $u = 0.635c$ in a 20 cm cavity is 7.5 mA, which seems practical for a real device.

V. CONCLUSION

We have made a quantum electrodynamic approach to analyze the basic radiation properties of the cavity CR radiation. Analytical expressions for the Einstein's A and B coefficients of the device are derived, which enable us to compare the Čerenkov radiation device with other radiation sources especially for the purpose of developing new radiation sources such as THz. We have shown that the Einstein's coefficients are profoundly modified by the cavity properties, and the coherent radiation is generated by the super radiation of spontaneous emission instead of stimulated emission. The theory has provided formula to calculate these effects and can be extended to explore more quantum effects for electrons in a cavity, in parallel to cavity QED.

ACKNOWLEDGMENT

The authors would like to thank P. D. Coleman for the discussion of his work on the Čerenkov radiation.

- [1] L. Mallet, C. R. Acad. Sci. Hebd Seances Acad. Sci. D **183**, 274 (1926).
- [2] P. A. Čerenkov, Compt. Rend. **2**, 451 (1934).
- [3] D. H. Perkins, *Introduction to High Energy Physics* (Addison-Wesley, Reading, 1982).
- [4] V. L. Ginzburg, J. Phys. (Moscow) **2**, 441 (1940).
- [5] P. D. Coleman and C. Enderby, J. Appl. Phys. **31**, 1699 (1960).
- [6] K. L. Felsh, K. O. Busby, R. W. Layman, D. Kapilow, and J. E. Walsh, Appl. Phys. Lett. **38**, 601 (1981).
- [7] D. S. Y. Hsu and J. Shaw, Appl. Phys. Lett. **80**, 118 (2002).
- [8] M. Abo-Bakr, J. Feikes, K. Holldack, P. Kuske, W. B. Peatman, U. Schade, G. Wustefeld, and H. W. Hubers, Phys. Rev. Lett. **90**, 094801 (2003).
- [9] G. Williams, Nature (London) **420**, 153 (2002).
- [10] E. R. Mueller, J. L. Hesler, T. W. Crowe, D. S. Kurtz, and R. M. W. II, in *Proceedings 2001 Space THz Technology Symposium* (2001).
- [11] R. Khler, A. Tredicucci, F. Beltram, H. E. Beere, E. H. Linfield, A. G. Davies, and D. A. Ritchie, Opt. Lett. **28**, 810 (2003).
- [12] P. Gu, M. Tani, S. Kono, K. Sakai, and X. C. Zhang, J. Appl. Phys. **91**, 5533 (2002).
- [13] I. M. Frank and I. Tamm, Compt. Rend. **14**, 109 (1937).
- [14] B. Johnson and J. E. Walsh, Phys. Rev. A **33**, 3199 (1986).
- [15] J. E. Walsh and J. B. Murphy, IEEE J. Quantum Electron. **8**, 1259 (1982).
- [16] G. B. Whitham, *Linear and Nonlinear Waves* (Wiley, New York, 1974).
- [17] L. Schachter, Phys. Rev. A **43**, 3785 (1991).
- [18] L. Schachter and J. A. Nation, Phys. Rev. A **45**, 8820 (1992).
- [19] J. Gao, Appl. Phys. Lett. (to be published).
- [20] E. Garate, R. Cook, P. Heim, R. W. Layman, and J. E. Walsh, J. Appl. Phys. **58**, 627 (1985).
- [21] R. Rohlsberger, K. Schlage, T. Klein, and O. Leupold, Phys. Rev. Lett. **95**, 097601 (2005).
- [22] V. B. Berestetskii, E. M. Lifshitz, and L. P. Pitaevskii, *Quantum Electrodynamics* (Butterworth, Heinemann, 1982).
- [23] R. H. Dicke, Phys. Rev. **93**, 99 (1954).